arXiv:1112.6429v1 [cond-mat.quant-gas] 29 Dec 2011

Anisotropic Ginzburg-Landau and Lawrence-Doniach Models for Layered Ultracold Fermi Gases

Mauro Iazzi,[1] Stefano Fantoni,[2] and Andrea Trombettoni[3,1]

[1] *SISSA, Via Bonomea 265, I-34136 Trieste, Italy*

[2] *ANVUR, P.za Kennedy 20, I-00144 Roma, Italy*

[3] *CNR-IOM DEMOCRITOS Simulation Center,*
Via Bonomea 265, I-34136 Trieste, Italy

We study the anisotropic Ginzburg-Landau and Lawrence-Doniach models describing a layered superfluid ultracold Fermi gas in optical lattices. We derive the coefficients of the anisotropic Ginzburg-Landau and the mass tensor as a function of anisotropy, filling and interaction, showing that near the unitary limit the effective anisotropy of the masses is significantly reduced. The anisotropy parameter is shown to vary in realistic setups in a wide range of values. We also derive the Lawrence-Doniach model - often used to describe the 2D-3D dimensional crossover in layered superconductors - for a layered ultracold Fermi gas, obtaining a relation between the interlayer Josephson couplings and the Ginzburg-Landau masses. Comparing to the Ginzburg-Landau description, we find that the region of validity of the Lawrence-Doniach model is near the unitary limit.

The presence and nature of the superfluid and superconducting transition in systems of different dimensionality is a widely studied and interesting topic. It is well known that the transition in two and three dimensions is radically different, as the first is governed by a Kosterlitz-Thouless mechanism of topological origin (the unbinding of vortices) and the second is the paradigmatic example of the symmetry breaking well described, at least qualitatively, by mean-field theories. This is the main reason of the wide interest in the study of materials with properties in-between the two, i.e. layered superfluids and superconductors. Their phenomenological properties are usually well described by anisotropic effective models: a successful example is given by the Lawrence-Doniach (LD) model [1] (in which the discrete layers are weakly coupled through Josephson terms) describing the electrodynamics of layered superconductors and copper oxides [2]. Another related way to introduce the effect of the layering is to consider a Ginzburg-Landau (GL) theory having anisotropic masses (eventually phenomenologically determined) [2]. A well known feature of these phenomelogical models is the fact that they work well even if the underlying microscopic mechanisms are not known (as it occurs for high-T_c cuprates).

In this paper we study and compare the anisotropic GL and LD models describing a layered superfluid ultracold Fermi gas in optical lattices: the coefficient of these phenomenological models can be microscopically derived and the parameters, like the strength of the optical lattices, can be tuned with high accuracy in realistic experimental setups. We determine the mass tensor in the GL theory as a function of anisotropy, filling and interaction, showing that near the unitary limit the effective anisotropy of the masses is significantly reduced. By tuning the strength of the optical lattices, the dimensionless anisotropy parameter γ in realistic setups can vary in a wide range of values: $\gamma \sim 1 - 200$ (for comparison with layered superconductors, we remind that $\gamma \sim 7$ for YBCO and $\gamma \gtrsim 150$ for BSCCO). We also derive the LD model, discussing a relation between the interlayer Josephson energy couplings in the LD model and the masses in the GL model. Using this result, the LD model with only couplings between adjacent planes is shown to be equivalent to the anisotropic GL theory in the BEC limit, while in the BCS side (where the size of the pairs is larger than the lattice spacing) next-nearest-neighbour couplings have to be taken into account.

Layered superconductors and superfluids: The first example of a layered superconductor was found in a naturally occurring compound of transition-metal dichalcogenides layers (such as TaS_2) intercalated with organic molecules [3], where, for temperatures of a few Kelvin, the metallic planes become superconductors. The discovery was followed later by the creation of artificial samples with alternating layers of different metals, having a different transition temperature [4]. The nature of the transition was found to be three dimensional [5], and the system was shown to be very well described by an anisotropic GL free energy at and above the transition, where the coherence length diverges as $\xi \propto (T - T_c)^{-1/2}$. At lower temperatures where the length ξ becomes comparable with the plane separation, the presence of a layer structure becomes important. To describe this Lawrence and Doniach proposed a tight-binding approximation [1] able to describe the crossover between the 2D behaviours of essentially decoupled planes to the 3D.

Another very important class of superconductors having a layered structure is the one of cuprates, discovered in 1986 by Bednorz and Müller [6]. Their characteristic structure presents a layer of one or more conducting copper oxide planes alternated to an insulating lattice with a perovskite-like structure. The layered structure makes the behaviour of cuprates strongly anisotropic and the dimensional crossover temperature is in general very near the critical temperature for the resistive transition [2]: despite the lack of a definitive consensus on the mechanism responsible for the superconductivity in the cuprates, it is by now established that the LD model successfully describe the transition and the electromagnetic response of cuprates [2, 7, 8].

The study of the dimensional crossover in cuprates is not in general an easy task: on one hand, the smallest barrier attainable is that of a single plane of an insulating material, on the other hand inserting several planes is a delicate process as the separation can become nonuniform [8].

From this point of view, ultracold atoms (and in particular ultracold fermions) in optical lattices provide a favourable setting: the tunnelling rate t can be controlled by adjusting the optical lattice parameters [9, 10] and the on-site energy coefficient U can be controlled through Feshbach resonances [11, 12]. The ratio U/t can be then controlled with high precision, as well as the geometry and the anisotropy of the system (e.g., optical lattices with different strengths can be superimposed in different directions). For ultracold bosons, optical lattices has been used to induce a Mott-insulator/superfluid quantum phase transition [13] and to study Josephson dynamics in many- and two- wells settings [14, 15]. The study of ultracold fermions in optical lattices also stimulated a huge amount of experimental work [16–21] and they provide a field of research in which even more far-reaching experiments are expected to take place. The low energy properties of ultracold fermions in deep optical lattices are described by Hubbard-like models [22]: metallic and insulating phases in 3D lattices have been studied [19, 20]. in presence of attractive interaction ($U < 0$) one has then a physical realization of the attractive Hubbard model [23–27].

Superimposing a 1D optical lattice to an ultracold Fermi gas gives raise to a stack of two-dimensional layers: very recently, the evolution of fermion pairing from 3D to 2D was experimentally studied, showing the opening of a gap in the radiofrequency spectrum when the dimensionality is reduced [21]. The confinement of Fermi mixtures in 2D was also experimentally investigated [28–33], showing properties different from the 3D case [34]. The observation of a pairing pseudogap in a 2D Fermi gas, using momentum-resolved photoemission spectroscopy, has been reported [33]. An important advantage of the use of an optical lattice is that when it is applied (say along the z direction) then the interlayer coupling $t_{\parallel}$ between 2D pancakes along z can be easily modified by varying the strength of the optical lattice. Furthermore, if two additional optical lattices are added in the xy plane, then the tunnelling $t_{\perp}$ can be tuned separately from $t_{\parallel}$ and the layering can be tuned by varying the ratio $t_{\parallel}/t_{\perp}$.

Effective models: Near the critical temperature, the superfluid wavefunction Ψ is small, so that the free energy difference δF between the normal and superfluid state can be expanded in powers of $|\Psi|^2$ [35]: for a layered superconductor/superfluid δF reads then

$$\delta F[\Psi] = \int d\vec{r} \left\{ \frac{\hbar^2}{2m_{\parallel}} (|\partial_x \Psi|^2 + |\partial_y \Psi|^2) + \frac{\hbar^2}{2m_{\perp}} |\partial_z \Psi|^2 + \alpha(T)|\Psi|^2 + \beta|\Psi|^4 \right\}. \qquad (1)$$

The phenomenological coefficients α and β appearing in (1) can be derived from experiments or from the microscopic Hamiltonian; the masses $m_{\parallel,\perp}$ are those of the Cooper pairs. The GL equations describing the equilibrium state can be found by minimizing (1) with respect to Ψ. For $\alpha > 0$ there is only the minimum $\Psi = 0$ corresponding to the normal state, while for $\alpha < 0$ there are uniform solutions $\Psi = |\Psi_0|e^{i\theta}$, hence the critical temperature is given by $\alpha(T_c) = 0$. In the LD tight-binding approach one has a 2D superfluid wavefunction $\Psi_n(x, y)$ for in the nth plane along z and the term with transverse derivative becomes $-J_1 \sum_n |\Psi_n(r) - \Psi_{n+1}(r)|^2$ with the nearest-neighbour tunnelling coefficient $J_1 \propto 1/d^2$ (d is the interlayer separation, i.e. the lattice spacing of the periodic potential along z).

In layered superconductors, the effects and the penetration of a magnetic field have been thoroughly studied [2, 7, 36]: such effects can be incorporated via the minimal substitution $\partial_i \to \partial_i - i\frac{e}{c}A_i$ (where $\vec{A}$ is the vector potential) and adding to the free energy the magnetization energy $F_H = (\vec{B} - \vec{H})^2/8\pi$. The penetration of the magnetic field in anisotropic type-II superconductors and the response of a layered superconductor to an electromagnetic field have been an established field of research for decades [2, 7, 36]. In the following we show that the layered GL theory (1) holds for a layered ultracold Fermi superfluid gas: then, to reproduce the phenomenology of the electrodynamics of layered superconductors in the context of ultracold atoms one can use a layered Fermi mixture in an fictitious magnetic field realized in a synthetic way using spatially dependent optical couplings between internal states of the atoms [37] or by rotating the trapping potential [38].

The Hamiltonian describing a two-component Fermi gas in a layered optical lattice reads $\hat{H} - \mu\hat{N}$, with the Hamiltonian $\hat{H}$ given by

$$\hat{H} = -\sum_{\langle ij\rangle\sigma}(t_{ij}\hat{\phi}^{\dagger}_{i\sigma}\hat{\phi}_{j\sigma} + h.c.) - U\sum_{i}\hat{\phi}^{\dagger}_{i\uparrow}\hat{\phi}_{i\uparrow}\hat{\phi}^{\dagger}_{i\downarrow}\hat{\phi}_{i\downarrow}, \tag{2}$$

where $\hat{N} = \sum_{i\sigma}\hat{\phi}^{\dagger}_{i\sigma}\hat{\phi}_{i\sigma}$ is the number operator, μ is the chemical potential, i, j are site indices, $\sigma = \uparrow, \downarrow$ is the spin index and $\hat{\phi}^{\dagger}_{i\sigma}$ is the fermionic operator (the sum is on distinct pairs of nearest-neighbours). The interaction is assumed attractive, $U > 0$, and the total number of fermions per site is denoted by n. The physical system modelled by (2) considers two optical lattices in the x, y directions (determining the tunnelling rate $t_{\parallel}$ between the sites in the xy planes) and a different lattice in the z direction, with interlayer coupling $t_{\perp}$. Notice that in our subsequent determination of the coefficients of the anisotropic GL and LD models the crucial ingredient is to have the optical lattice along z and the mechanism of layering in the form of tunnelling between adjacent layers: if the optical lattices in the x, y directions are absent (or small), then the anisotropic GL (1) is again obtained (with $m_{\parallel} = 2m$, where m is the mass of the fermionic atoms). Similarly, in writing (2) we assumed

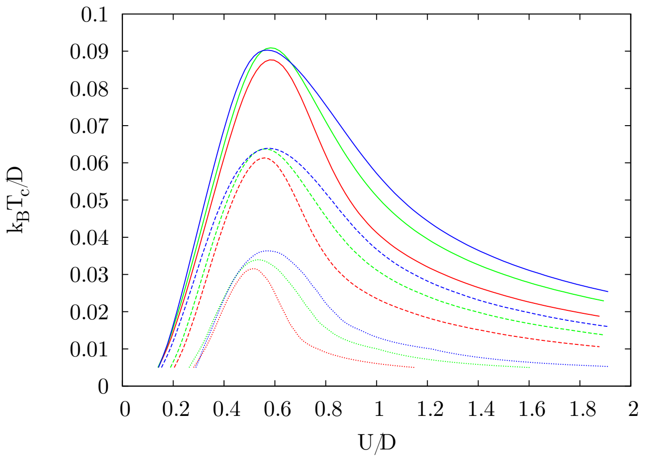

FIG. 1. Critical temperature k_BT_c as function of U (both scaled in units of the total bandwidth D) at various particle densities - $n = 0.9$ (solid lines), $n = 0.5$ (dashed lines), $n = 0.1$ (dotted lines) - and anisotropies $t_\perp/t_\parallel = 1,\ 0.3,\ 0.1$ (in each set from top to bottom).

that in each minimum of the lattice there is a total number of fermions $n \leq 2$ (i.e., only the lowest band of the periodic potential is occupied): otherwise, we would have a multi-band Hubbard model and again (1) would be retrieved.

The single-particle energies of Hamiltonian (2) for $U = 0$ are $\epsilon^{(0)}_{\vec{k}} = -2t_\parallel(\cos k_xd + \cos k_yd) - 2t_\perp \cos k_zd$ with total bandwidth $D = 8t_\parallel + 4t_\perp$. The isotropic 3D case corresponds to $t_\parallel = t_\perp$, while the isotropic 2D case to $t_\perp = 0$ (isolated pancakes). Estimates of the value of U for which the BCS-BEC crossover occurs gives $U \approx 0.7D$ in 3D and $U \approx 0.2D$ in 2D [23–27].

To derive the coefficients of the anisotropic GL we proceed in a path-integral setting [39–41]: performing the Hubbard-Stratonovich transformation and integrating out the fermionic field, a bosonic effective action is obtained (the critical temperature T_c is the one at which the order parameter is vanishing). Details are in Appendix A: the coefficients of the GL free energy (1) are found to be

$$\frac{\hbar^2}{2M_a} = \left[\sum_{\vec{k}}\left\{\beta^2 XY + \frac{\beta Y}{\epsilon_{\vec{k}}} - \frac{2X}{\epsilon^2_{\vec{k}}}\right\}\frac{(\partial_{q_a}\epsilon_{\vec{k}+\vec{q}})^2}{8\epsilon_{\vec{k}}} + \sum_{\vec{k}}\left\{\frac{X}{4\epsilon^2_{\vec{k}}} - \frac{\beta Y}{8\epsilon_{\vec{k}}}\right\}\partial^2_{q_a}\epsilon_{\vec{k}+\vec{q}}\right]_{\vec{q}=0}, \tag{3}$$

$$\alpha = \frac{1}{U} - \sum_{\vec{k}}\frac{X}{2\epsilon_{\vec{k}}}, \quad \beta = \sum_{\vec{k}}\left\{\frac{X}{4\epsilon^3_{\vec{k}}} - \frac{\beta Y}{8\epsilon^2_{\vec{k}}}\right\}: \tag{4}$$

in (3) $a = x, y, z$ denotes the direction and the mass parameters M_a are related to the masses in the GL energy (1) by $M_a = m_a U^2$ (with $m_x = m_y \equiv m_\parallel$, $m_z \equiv m_\perp$). It is $\epsilon_{\vec{k}} = \epsilon^{(0)}_{\vec{k}} - \mu$, $X = \tanh(\beta_c \epsilon_{\vec{k}}/2)$ and $Y = \cosh^{-2}(\beta_c \epsilon_{\vec{k}}/2)$.

It is also possible to derive the LD tunnelling coefficients: in the LD model, the xy layers are weakly coupled along the z direction through Josephson terms. Usually, only Josephson couplings between adjacent planes are considered. Here we consider the more general possibility of longer range tunnelling: this amounts to consider a Josephson contribution $-\sum_{n,m} J_{n,m} \mid \psi_n - \psi_m \mid^2$ to the energy, where n, m are denoting the different planes (i.e., the minima along z). We find

$$J_{n,m} = -\frac{U^2 d}{2\pi} \int dq_z e^{-i(n-m)q_z d} \chi(i\omega = 0; 0, 0, q_z) \tag{5}$$

where the expression for $\chi(q) = \chi(i\omega; \vec{q})$ is reported in Appendix A, Eq.(A10). In presence of lattices in the x, y directions, one can similarly define Josephson couplings $J^{\parallel}_{n,m}$. It is possible to determine a useful relation between the coefficients $J_{n,m}$ and the mass $m_\perp$ of the anisotropic GL model: one finds

$$\frac{\hbar^2}{2m_\perp d^2} = \sum_{p=1}^{\infty} p^2 J_p, \tag{6}$$

where we used the notation $J_p \equiv J_{n,n+p}$ (we are assuming translational invariance along z): then $J_1 = J_{n,n+1}$.

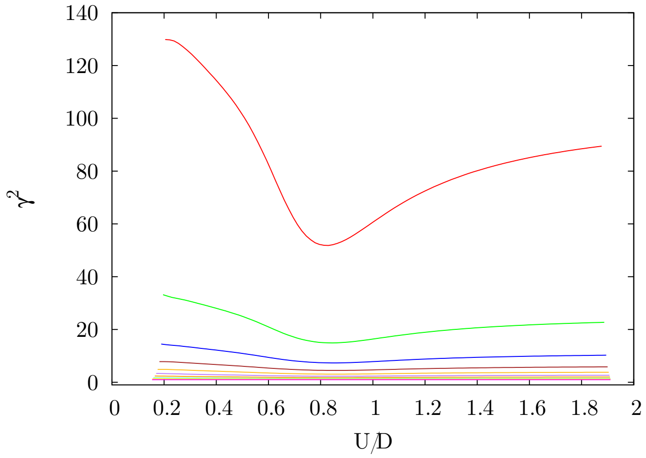

FIG. 2. Anisotropy parameter $\gamma^2 = m_\perp/m_\parallel$ vs. U/D for different anisotropies: from top to bottom $t_\perp/t_\parallel = 0.1$, 0.2, 0.3, 0.4, 0.5, 0.7, 0.7, 0.8, 0.9, 1 (with $n = 0.5$).

Results: The quantities X, Y entering Eqs. (3)-(4) depend on $\beta_c = 1/k_B T_c$: therefore in order to evaluate the masses $m_\parallel$, $m_\perp$ one has to determine T_c and μ as a function of the interaction U, the filling n and the anisotropy $t_\parallel/t_\perp$. In Appendix A we write the two equations from which we can determine T_c and μ. The results for the critical temperature T_c for various values of filling n and of the ratio $t_\perp/t_\parallel$ are plotted in Fig.1: we plot both T_c and U in units of D, showing that in these units the effect of the anisotropy is relatively small (the critical temperature in the interval $0.5 \lesssim t_\perp/t_\parallel \lesssim 1$ is very similar to the T_c of the isotropic case). The maximum value of the critical temperature occurs practically at the same value of the interaction when the total bandwidth D is used as energy unit.

Using the critical temperature T_c, we can compute the mass anisotropy parameter γ usually defined [2] as

$$\gamma^2 = \frac{m_\perp}{m_\parallel}. \tag{7}$$

The anisotropy parameter γ plays a crucial role in the electrodynamics of layered superconductors since a formula giving the value of a quantity for a general anisotropy parameter γ given its value for $\gamma = 1$ holds [42]. Values of γ for several superconducting compounds has been determined from experimental data [2]. In layered Fermi superfluids, the value of γ affects the critical value of a synthetic magnetic field (this is the atomic counterpart of the effect of a magnetic field on a layered superconductor [2]): supposing to have a general rotation

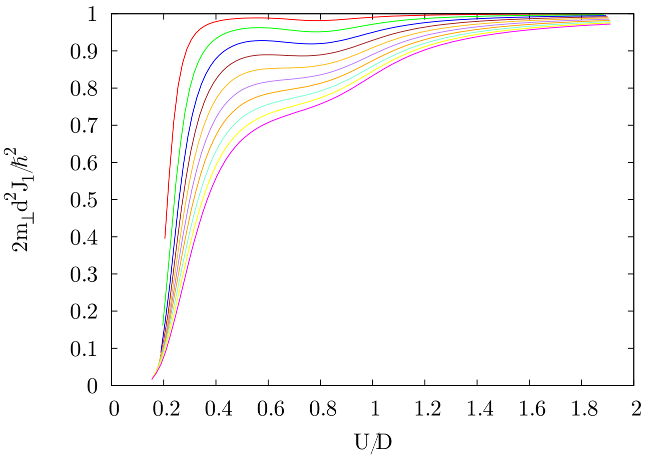

FIG. 3. Plot of the quantity $2m_\perp d^2 J_1/\hbar^2$ vs. U/D at $n = 0.5$ (with d lattice spacing) for the same values of $t_\perp/t_\parallel$ of Fig.2.

$\vec{\Omega}$, the critical values of the rotation for the vortex melting obey the relation $\Omega_{c2\|}/\Omega_{c2\perp} = \gamma$. The mass ratio could be experimentally determined from momentum-resolved photoemission spectroscopy [33] or from the measurement of the frequency of the collective excitations [34].

The results for the anisotropy parameter γ of a layered ultracold Fermi gas are shown in Fig.2: γ significantly decreases close to the unitary limit due to the effect of the increase of T_c in the crossover region. This result is consistent with the qualitative expectation that the effect of external anisotropies is softened in the unitary limit. Results for γ vs. filling are reported in Fig.5: the filling modifies γ on the BCS side, while the anisotropy on the BEC side remains virtually identical. To understand if and how much the collective behaviour enhances or not the (external) anisotropy artificially tuned by imposing a layering through a value of $t_\|/t_\perp$ smaller than one, we studied an *effective* anisotropy defined as $\gamma_{eff}^2 = \gamma^2 \cdot t_\perp/t_\|$. The results are drawn in Fig.6: it is seen that in the BCS side the enhancement is more pronounced with respect to the BEC side. Again, the effective enhancement is reduced in the unitary limit. We also checked that in the BEC limit the quantity $\gamma^2 \cdot (t_\perp/t_\|)^2$ is found to approach 1 for different fillings, see Fig.7.

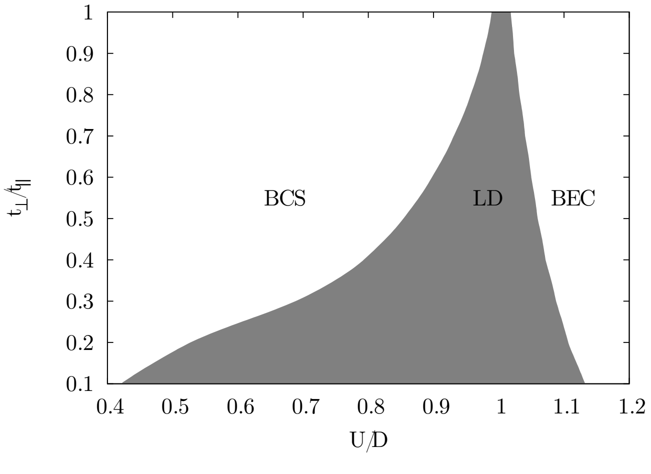

FIG. 4. Plot of the validity region of the LD model (with $n = 0.5$), obtained by fixing an arbitrary value $J_1^a = 0.8\frac{\hbar^2}{m_i d^2}$ at which we consider the Josephson tunnelling to be a good description of the pair motion along axis $a = x, y, z$ (here $J_1^x = J_1^y \equiv J_1^\|$ and $J_1^z \equiv J_1^\perp$). The shaded region is where the pairs move with discrete jumps in the z direction, but not in the x and y directions.

Finally, we numerically evaluated the LD coefficients (5) and compared them to the GL masses in Eq. (3). We found that in the BEC side the nearest-neighbour Josephson coupling J_1 is enough to give the correct value $m_\perp$, but not on the BCS side of the crossover, where the size of the pairs is significantly larger than d. Then, the anisotropic GL model is equivalent to the LD equations with the Josephson couplings J_1 only in the BEC regime (for arbitrary filling): using only nearest-neighbour Josephson couplings for the free energy instead of the continuous kinetic energy term in the direction z is approximately correct when $2m_\perp d^2 J_1/\hbar^2$ is near 1, as one can see from Eq. (6). The results in Fig.3 show a non-monotonous behaviour around the unitary limit. The validity region of the LD model with only Josephson couplings J_1 along z is seen to increase when the layering becomes stronger (i.e., $t_\perp/t_\parallel$ becomes smaller). In presence of lattices in the x, y directions, the use of the LD model is especially appropriate when the Josephson couplings can be used in the perpendicular directions (across the planes) but not in the parallel direction (between the planes). To give a qualitative idea of the interval where the LD model is valid one can choose an arbitrary threshold (we choose 0.8) and plot the region where $2m_\parallel d^2 J_1^\parallel/\hbar^2 < 0.8 < 2m_\perp d^2 J_1/\hbar^2$. As can be seen in Fig.4, the validity region of the LD model is narrower for small layering (i.e., $t_\perp/t_\parallel$ close to 1) and it is centered around the interval in which the critical temperature reaches its maximum value. This result is pictorially summarized in Fig.8.

Conclusions: In this paper we studied the superfluid phase of an ultracold layered Fermi gas in the presence of an optical lattice near the critical temperature. This system is described by an anisotropic Ginzburg-Landau theory (that is also used for other systems such as layered superconductors). We derived the coefficients of the Ginzburg-Landau equation: the anisotropy was shown to be enhanced by the superfluid, and the anisotropy parameter γ decreases near the crossover region. The dependence on filling was found to be important on the BCS side of the crossover and negligible when the gas is in the molecular condensate phase. These results link the underlying microscopic structure to the macroscopic properties of the superfluid: it is then possible to tune the experimentally controllable parameters such as interaction strength, filling and lattice strength in order to emulate the phenomenological electrodynamics of layered superconductors. We also derived the Lawrence-Doniach model for the layered ultracold Fermi gas and we discussed a relation between the interlayer

Josephson couplings in the Lawrence-Doniach model and the masses in the Ginzburg-Landau energy. Using this result, the Lawrence-Doniach model with only couplings between adjacent planes is shown to be valid in the crossover region between the BCS and the BEC limits.

Acknowledgments: Discussions with K. Schmidt and G. Roati are gratefully acknowledged.

Appendix A: Coefficients of the anisotropic Ginzburg-Landau model

In this Appendix we provide details and further results on the derivation and the study of the coefficients of the anisotropic GL equations for a layered superfluid Fermi gas, providing as well the equations giving the critical temperature T_c. The starting point is the Hubbard Hamiltonian (2):

$$\hat{H} = -\sum_{\langle ij \rangle \sigma} (t_{ij} \hat{\phi}^\dagger_{i\sigma} \hat{\phi}_{j\sigma} + h.c.) - U \sum_i \hat{\phi}^\dagger_{i\uparrow} \hat{\phi}_{i\uparrow} \hat{\phi}^\dagger_{i\downarrow} \hat{\phi}_{i\downarrow}, \tag{A1}$$

where $\hat{\phi}^\dagger_{i\sigma}$ is the fermionic operator, t_{ij} denote the tunnelling rates, μ is the chemical potential and $\sigma = \uparrow, \downarrow$ is the spin index. Furthermore i, j are site indices and $\hat{N} = \sum_{i\sigma} \hat{\phi}^\dagger_{i\sigma} \hat{\phi}_{i\sigma}$ is the total number operator. The interaction is assumed attractive, $U > 0$, and we denote by n the total number of fermions per site ($n \leq 2$). The tunnelling rate between the sites in the xy planes is denoted by $t_\parallel$, while the tunnelling rate along the z axis is denoted by $t_\perp$.

As discussed in the main text, in our study of the anisotropic GL and LD coefficients the crucial ingredient is to have the optical lattice along z and the mechanism of layering in the form of tunnelling between adjacent layers: with small (or absent) optical lattices in the x, y directions, then the anisotropic GL (1) would be obtained. In writing (A1) we also that in each site of the lattice there is a total number of fermions $n \leq 2$: otherwise, one has a multi-band Hubbard description and again the anisotropic GL would be retrieved.

In a path-integral setting the fermionic atoms are described by the independent Grassmann fields ϕ and $\bar{\phi}$ [39–41, 43, 44]: the partition function is given by $Z = \int \mathcal{D}\phi \mathcal{D}\bar{\phi} e^{-S_f[\phi,\bar{\phi}]}$, with S_f the fermionic action in imaginary time [40]. First, the Hubbard-Stratonovich transformation is performed by completing the Gaussian integral: the theory has then the form of a (free) fermion field interacting with the bosonic field Δ. The corresponding action reads

$$S = \sum_{kq} \bar{\Phi}_q^T (G_{kq}^{-1} + M_{kq}) \Phi_k - \beta\mu + \sum_{k-q} \frac{\bar{\Delta}_{k-q}\Delta_{k-q}}{U}, \tag{A2}$$

where

$$\Phi_k = \begin{pmatrix} \phi_{k\uparrow} \\ \bar{\phi}_{-k\downarrow} \end{pmatrix}, \tag{A3}$$

$$G_{kq}^{-1} = \delta_{kq} \begin{pmatrix} i\omega + \epsilon_{\vec{k}} & 0 \\ 0 & i\omega - \epsilon_{-\vec{k}} \end{pmatrix}, \tag{A4}$$

and

$$M_{qk} = \begin{pmatrix} 0 & \Delta_{k-q} \\ \bar{\Delta}_{q-k} & 0 \end{pmatrix} \tag{A5}$$

(here $\beta = 1/k_BT$, while in the main text it only denotes the coefficient of the quartic term in the GL free energy). In the previous formulas $\epsilon_{\vec{k}} = \epsilon_{\vec{k}}^{(0)} - \mu$ where $\epsilon_{\vec{k}}^{(0)} = -2t_\parallel(\cos k_x + \cos k_y) - 2t_\perp \cos k_z$ denote the single-particle energies (in this Appendix the lattice spacing is set to 1). Furthermore we used the notation $k = (i\omega; \vec{k})$ where the wavevectors $\vec{k}$ belong to the Brillouin zone $[-\pi; \pi]^3$ and $\omega_\ell = \ell\pi/\beta$ are the Matsubara frequencies (with ℓ even or odd in the case of bosons and fermions respectively). The sum over k corresponds to an integral over $\vec{k}$ over the Brillouin zone and sum over the integers ℓ; furthermore, $\phi_{j\sigma}(\tau) = \sum_k e^{i\left(\vec{k}\cdot\vec{r}_j - \omega_\ell\tau\right)} \phi_\sigma(i\omega_\ell; \vec{k})$ ($\vec{r}_j$ is the position of the site j).

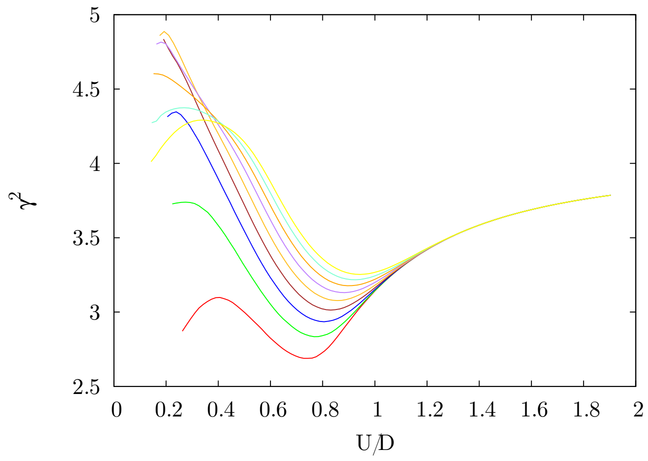

FIG. 5. Anisotropy parameter $\gamma^2 = m_\perp/m_\parallel$ vs. U/D at fixed $t_\perp/t_\parallel = 0.5$ and different particle densities n (from top to bottom $n = 0.1$, 0.2, 0.3, 0.4, 0.5, 0.6, 0.7, 0.8, 0.9).

The fermionic degrees of freedom can be integrated out obtaining the bosonic effective action

$$S = \mathrm{tr}\ln[G_{kq}^{-1} + M_{kq}] - \beta\mu + \sum_k \frac{\bar{\Delta}_k \Delta_k}{U}. \tag{A6}$$

The critical temperature T_c is the temperature for which the solution has $\Delta_0 = 0$ where $\Delta_0 = \langle\Delta\rangle$. When the interaction is weak, only the atoms around the Fermi level form Cooper pairs (BCS limit) [34]. In the BCS limit Cooper pairs have zero relative momentum, i.e. $\langle\Delta_k\rangle \approx 0$ for $k \neq 0$, and the chemical potential is not changed from the Fermi energy E_F. In this limit the phase-space integration can be done by saddle point approximation leading to the mean-field equations. The result is that $T_c \ll T_F$, where T_F is the Fermi temperature [34, 41]. When this is not the case, one has to consider the effects of higher order fluctuations [40] and solve two coupled equations to obtain μ and Δ_0 as a function of the interaction U, the hopping rates $t_\parallel$ and $t_\perp$, the particle density n and the temperature T. The first equation is the saddle point equation for the order parameter Δ_0:

$$\frac{1}{U} = \sum_{\vec{k}\in BZ} \frac{\tanh(\beta E_{\vec{k}}/2)}{2E_{\vec{k}}} \tag{A7}$$

where $E_{\vec{k}} = \sqrt{\epsilon_{\vec{k}}^2 + \Delta_0^2}$. The other is the number equation

$$n = -\frac{\partial}{\partial\mu} F \tag{A8}$$

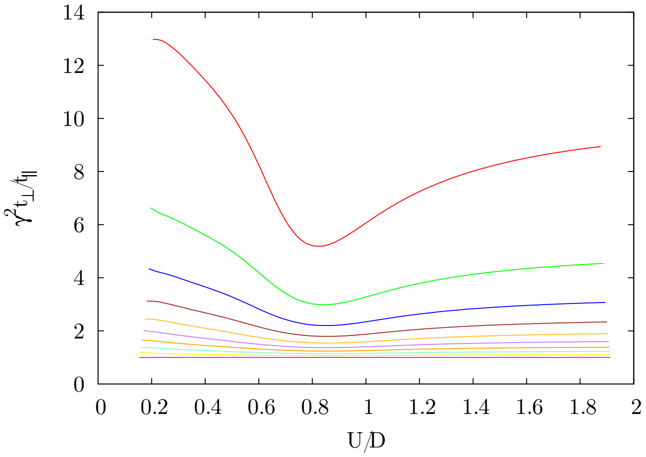

FIG. 6. Effective anisotropy γ_{eff}^2 as a function of U/D for different anisotropies (at $n = 0.5$): from top to bottom $t_\perp/t_\parallel = 0.1, 0.2, 0.3, 0.4, 0.5, 0.6, 0.7, 0.8, 0.9, 1$.

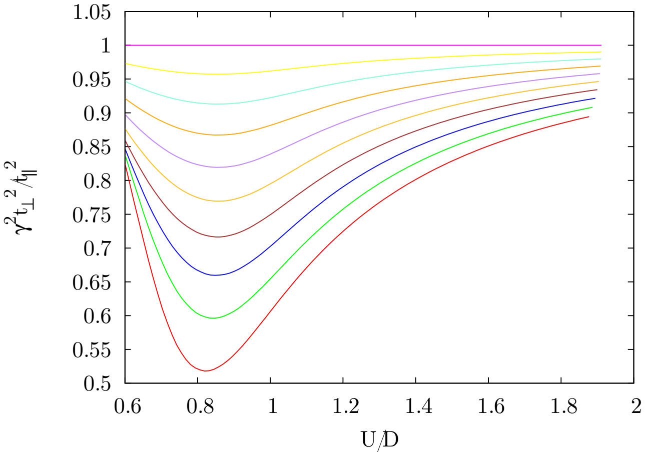

FIG. 7. Plot of $\gamma^2 \cdot (t_\perp/t_\parallel)^2$ vs. U/D at $n = 0.5$ for the same layering values $t_\perp/t_\parallel$ of Fig.6.

where (apart from a constant)

$$F = -\frac{1}{\beta} \sum_{\vec{k} \in BZ} \ln\left(1 + e^{-\beta \epsilon_{\vec{k}}}\right) + \frac{1}{\beta} \sum_q \ln \left\{ \frac{1}{U} + \chi(q) \right\} \tag{A9}$$

is the free energy and $\chi(q)$ is the pair polarization function, which for $\Delta_0 = 0$ reads

$$\chi(q) = \beta^{-1} \sum_k G_k^+ G_{k+q}^- \tag{A10}$$

with $G_k^\pm = \left(i\omega \pm \epsilon_{\vec{k}}\right)/(\omega^2 + \epsilon_{\vec{k}}^2)$.

To determine the critical temperature T_c one has to solve the two Eqs. (A7)-(A8) with $\Delta_0 = 0$: in this way one obtains T_c and μ as a function of the tunneling rates $t_\parallel$ and $t_\perp$, the particle density n and the interaction U. We observe that the numerical solution of (A7)-(A8) involves for the lattice case the explicit evaluation of (derivatives of) integrals over six variables, while in the 3D continuum case [39] one can exploit the rotational invariance and actually evaluate integrals in three variables. A simplification in the numerics is obtained noticing that after transforming the sum over Matsubara frequencies into a contour integral a first order pole appears that has to be corrected by either a limiting procedure putting $i\omega + 0^+$, or by subtracting the contour integral at infinity which can be obtained analytically. The solution of Eqs. (A7)-(A8) for T_c vs. U for different fillings and anisotropies is shown in Fig.1. One also observes that, as in the continuum case, the unitary point is different from the maximum T_c point.

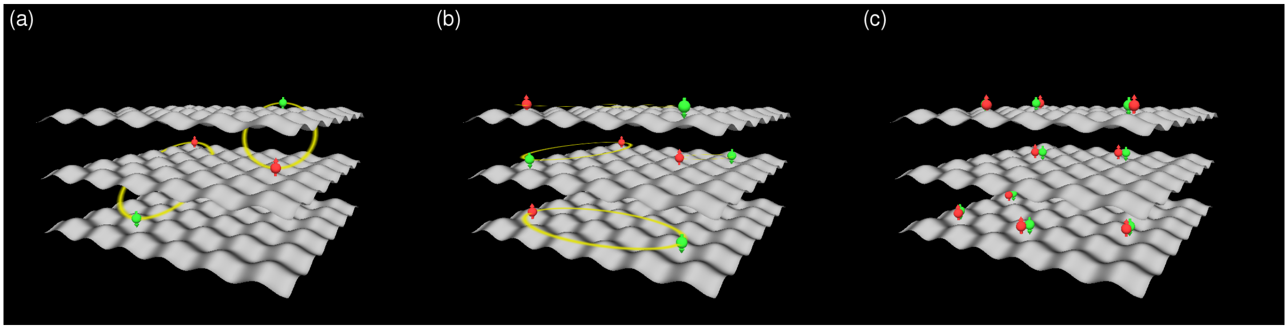

FIG. 8. The different regimes spanned by a layered superfluid: (a) in the BCS regime the Cooper pairs are spread both along and across the planes; (b) in the Lawrence-Doniach regime the Cooper pairs live each in one plane – having a large in plane radius – and tunnel between the layers as a single particle; (c) in the BEC regime each pair forms a tightly bound molecule and stays mostly in one site. As shown in Fig.4, the region where the Lawrence-Doniach model is important in the crossover between the BCS and BEC limits.

If the system is near the critical temperature T_c, the average value of Δ is small and the effective action can be expanded in series [39, 43]. Stopping at the fourth order gives

$$S - S_0 = \frac{1}{2}\,\mathrm{tr}(GMGM) + \sum_k \frac{\bar{\Delta}_k \Delta_k}{U} + \frac{1}{24}\,\mathrm{tr}[(GM)^4], \tag{A11}$$

where $S_0 = \ln\det(G^{-1}) - \beta\mu$ describes a non-interacting Fermi gas. The last step in finding a GL form for the action is to expand each coefficient around $\vec{q} = 0$ (time-dependence can be also included by expanding in $i\omega$). The resulting action is of the same form as the GL free energy (1), with the GL coefficients $m_\perp$, $m_\parallel$, α, β given in Eqs. (3)-(4).

We remark that the action just derived is also the free energy when the value $\langle\Delta\rangle$ is fixed. A natural question arises whether this functional corresponds to the original GL free energy, that is a functional of the anomalous correlation function. It can be seen that the minimum condition $\partial_\Delta F[\Delta] = 0$ gives $\langle\hat{\phi}_{i\downarrow}\rangle\ \langle\phi_\downarrow\phi_\uparrow\rangle = \Delta/U$, so that the free energy just found gives the correct equilibrium values for the observables.

Once that the GL coefficients $m_\perp$, $m_\parallel$, α, β are obtained (and their explicit evaluation requires the previous determination of T_c and μ), it is then possible to evaluate the anisotropy parameter $\gamma = \sqrt{m_\perp/m_\parallel}$. Our results for γ as a function of the interaction U at a fixed filling n are plotted in Fig.2. We also studied the influence of the filling on the anisotropy parameter: our findings are reported in Fig.5. The filling modifies γ on the BCS side, where the dynamics is determined by the atoms at the Fermi surface. On the other side of the unitary limit, the dynamics interests all the energy scales and is less susceptible to filling. In particular while the critical temperature for a given interaction value U increases with filling, the anisotropy on the BEC side remains virtually identical.

A natural question is whether the collective behaviour enhances or not the anisotropy that is artificially tuned by imposing a layering through a value of $t_\parallel/t_\perp$ smaller than one: for this reason we define an *effective* anisotropy γ_{eff} defined through the relation

$$\gamma_{eff}^2 = \gamma^2 \frac{t_\perp}{t_\parallel} = \frac{m_\perp}{m_\parallel} \frac{t_\perp}{t_\parallel}. \tag{A12}$$

The reason behind the choice of the definition (A12) is that we expect that the effective mass along the direction a is $\sim 1/t_a$ (where $a = x, y, z$). Then a value of γ_{eff} larger than one signals an effective enhancement of the anisotropy (with respect to the "external" anisotropy $t_\parallel/t_\perp$). The results are drawn in Fig.6: it is seen that in the BCS side the enhancement is more pronounced with respect to the BEC side. Again, the effective enhancement is reduced in the unitary limit.

The pair tunnelling in the BEC limit is expected to approach the strong coupling value $t_{\parallel,\perp}^2/U$ for each direction. Indeed in the BEC limit the quantity $\gamma^2 \cdot (t_\perp/t_\parallel)^2$ is found to approach 1 (with the convergence to the BEC limit being slower for systems with stronger layering), as shown in Fig.7.

Finally, in Fig.8 we pictorially depict the physical regimes of a layered ultracold Fermi gas.

---

[1] W.E. Lawrence and S. Doniach, in *Proc. 12th Int. Conf. Low Temp. Phys.*, ed. E. Kanda, 361 (Tokyo, Keikagu, 1971).

[2] M. Tinkham, *Introduction to superconductivity* (New York, McGraw-Hill, 1996).

[3] F.R. Gamble, F.J. DiSalvo, R.A. Klemm, and H.T. Geballe, Science **168**, 568 (1970).

[4] S.T. Ruggiero, T.W. Barbee, and M.R. Beasley, Phys. Rev. Lett. **45**, 1299 (1980).

[5] R.A. Klemm, A. Luther, and M.R. Beasley, Phys. Rev. B **12**, 877 (1975).

[6] J.G. Bednorz and K.A. Müller, Z. Phys. B **64**, 189 (1986).

[7] G. Blatter, M.V. Feigel'man, V.B. Geshkenbein, A.I. Larkin, and V.M. Vinokur, Rev. Mod. Phys. **66**, 1125 (1994).

[8] A.J. Leggett, Nature Phys. **2**, 134 (2006); *Quantum liquids: Bose condensation and Cooper pairing in condensed-matter systems*, Chap. 7 (Oxford, Oxford University Press, 2006).

[9] O. Morsch and M.K. Oberthaler, Rev. Mod. Phys. **78**, 179 (2006).

[10] I. Bloch, J. Dalibard, and W. Zwerger, Rev. Mod. Phys. **80**, 885 (2008).

[11] L.P. Pitaveskii and S. Stringari, *Bose-Einstein condensation* (Oxford, Clarendon Press, 2003).

[12] C.J. Pethick and H. Smith, *Bose-Einstein condensation in dilute alkali gases* (Cambridge, Cambridge University Press, 2008).

[13] M. Greiner, O. Mandel, T. Esslinger, T.W. Hansch, and I. Bloch, Nature **415**, 39 (2002).

[14] F.S. Cataliotti, S. Burger, C. Fort, P. Maddaloni, F. Minardi, A. Trombettoni, A. Smerzi, and M. Inguscio, Science **293**, 843 (2001).

[15] M. Albiez, R. Gati, J. Fölling, S. Hunsmann, M. Cristiani, and M.K. Oberthaler, Phys. Rev. Lett. **95**, 010402 (2005).

[16] G. Modugno, F. Ferlaino, R. Heidemann, G. Roati, and M. Inguscio, Phys. Rev. A **68**, 011601 (2003).

[17] J.K. Chin, D.E. Miller, Y. Liu, C. Stan, W. Setiawan, C. Sanner, K. Xu, and W. Ketterle, Nature **443**, 961 (2006).

[18] T. Stöferle, H. Moritz, K. Günter, M. Köhl, and T. Esslinger, Phys. Rev. Lett. **96**, 030401 (2006).

[19] U. Schneider, L. Hackermuller, S. Will, T. Best, I. Bloch, T.A. Costi, R.W. Helmes, D. Rasch, and A. Rosch, Science **322**, 1520 (2008).

[20] R. Jordens, N. Strohmaier, K. Gunther, H. Moritz, and T. Esslinger, Nature **455**, 204 (2008).

[21] A.T. Sommer, L.W. Cheuk, M.J.-H. Ku, W.S. Bakr, and M.W. Zwierlein, arXiv:1110.3058

[22] W. Hofstetter, J.I. Cirac, P. Zoller, E. Demler, and M.D. Lukin, Phys. Rev. Lett. **89**, 220407 (2002).

[23] J.M. Singer, M.H. Pedersen, T. Schneider, H. Beck, and H.G. Matuttis, Phys. Rev. B **54** 1286 (1996).

[24] A. Sewer, X. Zotos, and H. Beck, Phys. Rev. B **66**, 140504 (2002).

[25] A. Toschi, P. Barone, M. Capone, and C. Castellani, New J. Phys. **7**, 7 (2005).

[26] E. Burovski, N. Prokof'ev, B. Svistunov, and M. Troyer, New J. Phys. **8**, 153 (2006).

[27] C.C. Chien, Q.J. Chen, and K. Levin, Phys. Rev. A **78**, 043612 (2008).

[28] K. Günter, T. Stöferle, H. Moritz, M. Köhl, and T. Esslinger, Phys. Rev. Lett. **95**, 230401 (2005).

[29] X. Du, Y. Zhang, and J.E. Thomas, Phys. Rev. Lett. **102**, 250402 (2009).

[30] K. Martiyanov, V. Makhalov, and A. Turlapov, Phys. Rev. Lett. **105**, 030404 (2010).

[31] B. Fröhlich, M. Feld, E. Vogt, M. Koschorreck, W. Zwerger, and M. Köhl, Phys. Rev. Lett. **106**, 105301 (2011).

[32] P. Dyke, E. D. Kuhnle, S. Whitlock, H. Hu, M. Mark, S. Hoinka, M. Lingham, P. Hannaford, and C. J. Vale, Phys. Rev. Lett. **106**, 105304 (2011).

[33] M. Feld, B. Fröhlich, E. Vogt, M. Koschorreck, and M. Köhl, Nature **480**, 75 (2011).

[34] S. Giorgini, L.P. Pitaevskii, and S. Stringari, Rev. Mod. Phys. **80**, 1215 (2008).

[35] V.L. Ginzburg and L.D. Landau, Zh. Eksp. Teor. Fiz. **20**, 1064 (1950).

[36] B. Rosenstein and D. Li, Rev. Mod. Phys. **82**, 109 (2010).

[37] Y.J. Lin, R.L. Compton, K. Jimenez-Garcia, J.V. Porto, and I.B. Spielman, Nature **462**, 628 (2009).

[38] A.L. Fetter, Rev. Mod. Phys. **81**, 647 (2009).

[39] C.A.R. Sa de Melo, M. Randeria, and J.R. Engelbrecht, Phys. Rev. Lett. **71**, 3202 (1993).

[40] M. Randeria, in *Bose-Einstein condensation*, eds. A. Griffin, D.W. Snoke, and S. Stringari, (Cambridge, Cambridge University Press, 1995).

[41] *The BCS-BEC Crossover and Unitary Fermi Gas*, ed. W. Zwerger (Heidelberg, Springer, 2012).

[42] G. Blatter, V.B. Geshkenbein, and A.I. Larkin, Phys. Rev. Lett. **68**, 875 (1992).

[43] M. Drechsler and W. Zwerger, Annalen der Physik **1**, 15 (1992).

[44] F. Pistolesi and G.C. Strinati, Phys. Rev. B **53**, 15168 (1996).